Indian Journal of Ecology (2023) 50(2): 289-305
DOI: https://doi.org/10.55362/IJE/2023/3893

Manuscript Number: 3893
NAAS Rating: 5.79

Prediction of Global Distribution of *Ganoderma lucidum* (Leys.) Karsten: A Machine Learning Maxent Analysis for A Commercially Important Plant Fungus

Manish Mathur and Preet Mathur[1*]

ICAR- Central Arid Zone Research Institute, Jodhpur-342 003, India
[1]Jodhpur Institute of Engineering and Technology, Jodhpur-342 802, India
**E-mail: preetm9535@gmail.com*

***Abstract*:** The global habitat suitability of the fungus *Ganoderma lucidum* was simulated using the Maxent machine learning technique in relation to a number of environmental factors. 1159 geographically thinned *G. lucidum* presence points were projected over three bio-climatic time frames: current, 2050 and 2070, using four representative concertation paths (RCPs), namely 2.6, 4.5, 6.0 and 8.5 along with few non-climatic variables like eecosystem rooting depth and rooting zone water storage size and ssurface soil characteristics. With these climatic and RCPs projections, areas under the receiver operating curve (AUC) were reached 0.90, suggested the excellent predictive qualities of the modelling. Based on Maxent output, habitat suitability types were identified using the ARC-GIS raster calculator tool, which provided optimum, moderate, marginal, and low suitability classes. The largest optimum habitat for this fungus was detected during current bioclimate time-frame, measuring 2983977.56 square kilometres, while smallest area (600355.52 square kilometres) under this niche type was recoded under 2050 RCP 6.0. By doing so, percent changes in each habitat class from their respective current to future projections were estimated and our analysis revealed -41.82 to -79.88 percent reduction for the optimum habitat areas. The Permutation Importance value indicated that energy/temperature variables have a much greater influence on this species' global niche distributions than do water variables, and these variables were identified as important predisposing factors for this fungus. Secondary predisposing variables for this fungus included an eight-centimetre ecosystem rooting depth and soil organic carbon levels of up to 145 (g/kg). From present study, it can deduce that this fungus is always present in specific European countries. However, both optimum and moderate habitat suitability for this species will deteriorate within Asian countries, making wild collection for various medicinal product synthesis more difficult. As a result, its availability in such areas will be heavily reliant on its in-vitro conditions (substratum) as well as the adjustment of micro-environmental variables identified in this work.

***Keywords*:** *Ganoderma lucidum,* Ecological Niche Modelling, Maxent analysis, Bio-climatic variables

Ganoderma is a genus of white-rot polypore fungi in the Ganodermataceae family that is distinguished by the development of a double-walled, generally echinulate basidiospore. *Ganoderma lucidum* can be found all over the world (Oke et al 2022). *G. lucidum* has been recognized as the major pathogen on tree species such as *Quercus spp., Cocos nucifera, Camellia sinensis, Prunus persica, Prosopis cineraria, Acacia tortalis, A. senegal, A. nilotica, A. catechu, Albizia lebbeck, Azardirachta indica, Casuarina equisetifolia.* Basal rot has killed *Prosopis cineraria* and *Acacia tortalis* trees in India's dry and semi-arid regions (Schuch and Kelly, 2007, Bhansali 2012) (Fig. 1). Despite being a wood-rotting mushroom, it also has antibacterial, antifungal, and antiviral (especially against herpes and HIV) as well as anticancer, anti-inflammatory, antioxidant, and radical scavenging qualities (Sudheer et al 2019). *G. lucidum* supplements are being marketed as food and medication supplements to improve immune system and metabolic performance. Frequently sold items include coffee, powdered tea, dietary supplements, beverages, syrups, toothpastes, soaps, and other similar products (Singh et al 2013). Because *Ganoderma* extract inhibits the tyrosinase enzyme, which stops the skin from producing melanin, it can be found in a variety of facial and cosmetic products (Hyde et al 2010). Due to its ability to reduce dihydrotestosterone and prostatic hyperplasia, it is also used to improve male hair (Meehan, 2015). Around 200 *Ganoderma* medications and over 1,000 other products are available (Chan et al 2021). Products made from *G. lucidum* are thought to be sold for more than 2.5 billion USD annually in Asian nations like China, Japan, and South Korea (Bijalwan et al 2020).

The market for nutraceuticals based on *Ganoderma* is expanding quickly in India, and is expected to reach $25 million USD in 2023 (El Sheikha et al 2022, Fatima et al 2022, Bijalwan et al 2021). On online marketplaces like Amazon, Flipkart, and others, a variety of genuine and verified *Ganoderma*-based products are readily available (www.vegamebeljepara.com; www. dazzlinggroup.com; www.dxnmalaysia.com and www.vegamebeljepara.com; Wu et al 2018). Figures 1d and 1e exhibit *G. lucidum*

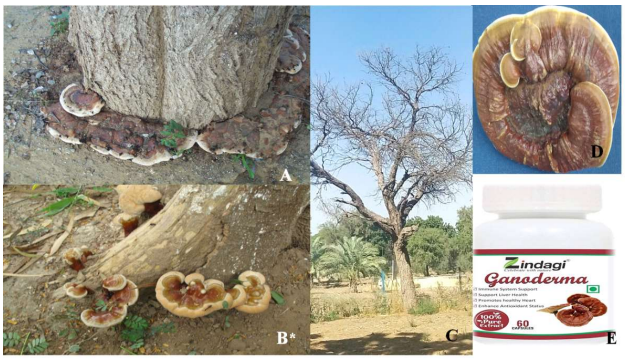

Fig. 1. *Ganoderma lucidum* on *Prospois cineraria* (A) and on *Acacia tortalis* (B*: photo courtesy by Dr. R.K. Bhansali). Dying of tree with infection of *G. lucidum* (C), fruiting bodies collected from filed (D) and health care product with *G. lucidum* as an active ingredient: E, https://vegandukan.com/products/zindagi-ganoderma-pure-extract-capsules-helpful -in-weight-loss-increase-energy-stamina?variant=39433736552634&currency=INR&utm_medium=product_sync&utm_source=google&utm_content=sag_organic&utm_campaign=sag_org (Jhanil Healthcare Pvt Ltd)

basidiocarps and its commercial product. There has been an effort to artificially cultivate this fungus due to the difficulty in finding it in the wild and the rising demand for its raw material on the global market (Bijlwan et al 2021). *G. lucidum* is primarily produced by solid-state fermentation, and the fruiting body develops over the course of about six months (Magday et al 2017). Alternative methods of fungi cultivation are required because the process is cumbersome and difficult to control (Yang et al 2019, Subedi et al 2021).

This ecological niche modelling was done with the help of the machine learning Maxent tool, which is a non-parametric Java-based application. From such analysis it was anticipated that such test facilitate scientific communities to understand how much space on the world is suitable for this species to grow in, based on bioclimatic and soil factors, as well as other factors related to rooting depth, total plant accessible water storage capacity. The study's findings add to the concern over how much *G. lucidum* material will be available from the wild under various climate change and greenhouse gas scenarios, which may be related to the need for its *in-vitro* production to meet industrial demands.

MATERIAL AND METHODS

Data collections: Distributional records for *G. lucidum* were obtained from data repositories such as the Global Biodiversity Information Facility (www.gbif.org/), the Indian Biodiversity Portal (https://indiabiodiversity.org/species/show/33318), published literature (Khara 1993, Khara and Singh 1997, Pilotti, 2005, Bhansali 2012, Basnet et al 2017, Bijalwan et al 2021, Shah et al 2021) and from field-based inventories (Jindal et al 2009 and 2010). The coordinates of these sites were identified on a WGS84 coordinate datum system using high-resolution Google Earth satellite image data and GIS ArcMap (Coban et al 2020) software. Furthermore, where occurrence data was unavailable, exact geo-coordinates were obtained by determining latitude and longitude values using Google Earth (http://ditu.google.cn/). Using the aforementioned sources, the distributional localities were assembled into a CSV database (.csv). To reduce spatial autocorrelation and duplicate records, and filtered our data set using the Spatial Thin window of the R-based Graphical User Interface Wallace Software (Kass et al 2018) with a thinning distance of 10 kilometers.

Bio-Climatic (BC) and non-bioclimatic variables: Based on where species are now, machine learning approaches can predict where they will be in the future (Phillips and Dudik 2008, Mathur and Mathur 2023). The bioclimatic variables used to estimate current and future distributions were taken from observational data in WorldClim ver. 1.4, which may be found online at https://worldclim.org/data/cmip6/cmip6clim30s.html (accessed on 21st August, 2022). 19 bioclimatic variables (Hijmans et al 2001, Kass et al 2018) were downloaded and converted to ASCII (or ESRI ASCII) in DIVA-GIS version 7.5 (Coban et al 2020, Ye et al 2020) for current as well as two future climatic scenarios (2050-time frame that represents the mean values from 2041 to 2060 and 2070-time frame that represents the mean values from 2061 to 2080 (Zhang et al 2021). These were downloaded pertains to four RCPs, namely RCP 2.6, RCP 4.5, RCP 6.0 and RCP 8.5. Details of each bio-climatic parameter, along-with their units and mathematical expressions are presented in Table 1.

Seven different soil parameters (bulk density kg/cm^3, cation exchange capacity cmol kg^{-1}, soil pH H_2O, sand percent, silt percent, clay percent contents, soil organic carbon stock g kg^{-1} and soil Nitrogen cg/kg from surface soil) were downloaded from the ISRIC World Soil Information database https://isric.org/soilgrids (Accessed on 15th August 2022). These data sets were obtained and processed through WMS servers using ArcMap. (Full instructions are available at https://www.isric.org/instruction-wms.html Cotrina Sánchez et al 2020).

Terrestrial Observation Panel for Climate of the Global Climate Observation System (GCOS) identified the 95% rooting depth as a key variable needed to quantify the interactions between the climate, soil, and plants. International Land Surface Climatology Project (ISLSCP) provided the data on vertical root distribution that encompasses data points from various land covers like

(evergreen needleleaf forest, evergreen broadleaf forest, deciduous broadleaf forest, mixed forest, wooded grassland, cropland, urban built-up and open shrubland, closed shrubland, bare ground (Schenk et al 2009). Data on this parameter was downloaded from http://daac.ornl.gov

ISLSCP II: total plant-available soil water storage capacity of the rooting zone provides estimates of the geographic distribution of the total plant-available soil water storage capacity of the rooting zone (rooting zone water storage size) on a 1.0^0 global grid (Kleidon 2011) https://daac.ornl.gov/ISLSCP_II/guides/root_water_storage_1deg.html. In the present study, utilized rooting zone water storage (mm H_2O) derived from assimilation of NDVI-fPAR (fraction of Absorbed Photosynthetically Active Radiation) and atmospheric forcing data. Further data-set on global croplands and pasture lands were downloaded and utilized as per the procedure provided by Ramankutty et al (2010a and b).

Issue of multicollinearity: The Pearson Correlation Coefficient (r) was used to investigate cross-correlation, and a multicollinearity test was run to check for over-fitting. In addition, variables with cross correlation coefficient values larger than or equal to 0.85 were gradually removed (Pradhan 2016) using the Niche Tool Box (Osorio-Olivera et al 2020 https://github.com/luismurao/ntbox). Following the procedures recommended by Kumar et al (2006), multi-collinearity among predictor variables was decreased. One significantly cross-correlated variable that is biologically relevant to the species and makes model interpretation simple was chosen from two others (Padalia et al 2014; Mathur and Mathur, 2023). For instance, it was found that the variables yearly precipitation and precipitation of the wettest month had a strong correlation, then chose to keep the latter variable because it depicts seasonal variability in precipitation. For further analysis, only one variable from each group of strongly correlated variables ($r^2 > 0.85$) was preserved. In this study, model training and model validation were assigned to 70% and 30% of the data, respectively (Obiakara and Fourcade 2018).

Projection correction: Because the Bio-Climatic (BC) and Non-BC variables were obtained from different sources and at different resolutions, their projections should be corrected before extracting data and predicting the ensemble model. This was accomplished through the use of a series of steps in ArcMap using ArcToolbox. First, defined the projection in Data Management Tools' "projection and transformation" sub-window then used the WGS 1984 EASE Grid Global Projected Coordinate System for this. Using the Raster Project Tab, the

Table 1. Predictive variables (Current and future) bio-climatic data variables. Calculation criterion of each variable (https://pubs.usgs.gov/ds/691/ds691.pdf)

Code	Environmental variables	Scaling factor	Unit
BC-1	Annual mean temperature	10	°C
BC-2	Mean diurnal range (Mean of monthly (max temp - min temp)	10	°C
BC-3	Isothermality (BC2/BC7) (×100)	100	Per cent
BC-4	Temperature seasonality (standard deviation ×100)	100	-
BC-5	Max temperature of warmest month	10	°C
BC-6	Min temperature of Coldest Month	10	°C
BC-7	Temperature annual range (BC 5-BC 6)	10	°C
BC-8	Mean temperature of wettest quarter	10	°C
BC-9	Mean temperature of driest quarter	10	°C
BC-10	Mean temperature of warmest quarter	10	°C
BC-11	Mean temperature of coldest quarter	10	°C
BC-12	Annual precipitation	1	mm
BC-13	Precipitation of wettest month	1	mm
BC-14	Precipitation of driest month	100	mm
BC-15	Precipitation seasonality (Coefficient of variation)	1	Per cent
BC-16	Precipitation of wettest quarter	1	mm
BC-17	Precipitation of driest quarter	1	mm
BC-18	Precipitation of warmest quarter	1	mm
BC-19	Precipitation of coldest quarter	1	mm

first step's output was reprojected with the same coordinate system, as well as the default resampling technique (Nearest neighbour assignment) and output cell size.

Species distribution modelling: In this study, the Maxent 3.4.1 software (http://www.cs.princeton.edu/schapire/Maxent/) was used to simulate and predict the potential geographical distribution probability of *G. lucidum* under current and two futures (2050- and 2070-time frame) scenarios (Coban et al 2020, Ye et al 2020). During the modelling process, 70% of the 1159 *G. lucidum* distribution data samples were randomly selected as training data, while 30% were used as testing data. The number of background points generated at random, was set to 10,000 (Zhang et al 2021). To avoid over-fitting of the test data, set the regularization multiplier to 0.1. (Phillips et al 2006) and used linear, quadratic, and hinge properties. A total of 100 runs were planned for model building (Flory et al 2012). In the environment parameter settings, Jackknife method was applied, and the other parameter settings were left at the software defaults. The performance of this model was evaluated based on the computed receiver operating characteristic (ROC) curve and the area under the curve (AUC). In general, AUC values vary from 0.5 to 1, which could be divided into five classes: fail (0.5–0.6), poor (0.6–0.7), fair (0.7–0.8), good (0.8–0.9), and excellent (0.9–1, Zhao et al 2021). The closer the AUC value was to 1, the farther away from the random distribution, the greater the correlation between environmental variables and the predicted geographical distribution of species, and the more accurate the performance of the model, while AUC < 0.5 is a contingency difference, which can be regarded as a stochastic forecasting model, and rarely happens (Hanley and McNeil 1982).

Post Ensemble Analysis

Habitat suitability: Raster outputs (ASCII) of the Maxent model were imported to ArcMap, and distinct habitat types for this species were defined based on their cell values (0 to 1). Follow the criteria of constant point break for each class (Khan et al 2022) kept a, resulting in four suitability classes: optimum, moderate, marginal, low and absent or inappropriate. Area (sq. km.) under these classes was quantified by using the raster calculator tool (spatial Analyst Tool/Map Algebra/Raster Calculator). To figure out how the different climate scenarios would affect the predicted habitat suitability, used the following formula to measure the percent change in mean habitat suitability under optimum class (Mathur, 2014a, Wright et al 2016, Kaky et al 2020).

$$\left[\left(\frac{\text{Future - Current}}{\text{Current}}\right)\times 100\right]$$

RESULTS AND DISCUSSION

Data processing and multicollinearity: The 1686 records were collected for this species from various sources around the world, and filtered out all but one occurrence of a specific record in a given location using the Spatial Thin window of R language-based Wallace Software's (Kass et al 2018) with a thinning distance of 10 kilometers. To complete the ENM development process, 1159 reports of the presence of *G. lucidum* were gathered. Results of correlation analysis among different bioclimatic variables are presented in Table 2. To address the issue of multicollinearity in species distribution modelling, employ the approaches proposed by Kumar et al (2006) and Pradhan et al (2016). BC-2 and BC-19 were significantly correlated with other bioclimatic variables during current and all predictive RCPs with 2050 and 2070. Precipitation of Warmest Quarter (BC-18) was the least correlative with other BC variables and hence that was utilized for ENM analysis of this species with all RCPs. Such trends were also recorded with Isothermality (BC-3) and Mean Temperature of Wettest Quarter (BC-8) except 2050 RCP 2.6 and 2070 RCP 8.5, respectively. Contrary to above trends, Annual Mean Temperature (BC-1) and Temperature Seasonality (BC-4) were utilized for analysis only during 2050 RCP 2.6. Among soil variables, CEC, nitrogen and silt contents exhibits significant correlations with other variables and hence, they were eliminated from further analysis.

The analysis of omission-commission plots demonstrates the effect of cumulative threshold selection on anticipated area as well as autocorrelation of sample points (test and training). The omission rate of the test sample should ideally be similar to the projected omission rate (Djebbouri et al 2021). Trends in such graphs can be explained by two criteria: higher omission rates on test samples than expected omission rates, showing independence between test and training data. Such findings show that spatial autocorrelation has no influence on the models. In certain cases, the test omission line is significantly lower than the predicted omission line, indicating that the test and training data are not independent and are derived from the same spatially autocorrelated presence data.

In this study, majority of predictors, our test omission lines are well matched with projected omission (Fig. 2), indicating that there is no autocorrelation in sampling and that our model attributes are not affected by sampling bias. However, for some variables, like as surface soil properties, 2050 RCP 4.5 and 2070 RCP 8.5 omission test lines are lower than the projected omission line showed some form of spatial association.

Predictors contributions: With 30.9% and 33% permutation relevance, annual precipitation (BC-12) was

determined as the most important controlling element for this species during current and 2050-RCP 4.5. Similarly, for 2050 RCP 6.0 and 8.5, the minimum temperature of the coldest month (BC-6) has the largest permutation relevance of 40.7 and 35.9%, respectively. The isothermality (BC-3) is the most essential factor for this species during 2070, with RCP 2.6 (40.3%), 4.5 (38.8%), and 6.0 (30.5%) being the greatest permutation importance values for the three greenhouse scenarios (Table 3). Temperature Seasonality (BC-4) with 37.7% PI and Precipitation of Wettest Quarter (BC-16) with

Table 2. Outputs of multi-collinearity tests conducted for different climatic data-sets. √ = use for analysis and x remove from analysis as they have significant correlation with other variables

Variables	Current	2050				2070			
		RCP 2.6	RCP 4.5	RCP 6.0	RCP 8.5	RCP 2.6	RCP 4.5	RCP 6.0	RCP 8.5
BC-1	x	√	x	x	x	x	x	x	x
BC-3	x	x	√	√	√	√	√	√	√
BC-4	x	√	x	x	x	x	x	x	x
BC-5	√	x	√	√	√	√	√	x	√
BC-6	√	x	√	√	√	x	x	√	x
BC-7	√	√	x	x	x	√	√	x	x
BC-8	x	√	√	√	√	√	√	√	x
BC-9	x	x	√	√	√	√	x	√	x
BC-10	x	x	x	x	√	x	x	√	x
BC-11	√	x	x	x	x	x	x	√	x
BC-12	√	√	√	x	x	x	x	x	x
BC-13	√	x	x	x	x	x	√	√	x
BC-14	x	√	√	√	x	√	x	√	√
BC-15	√	x	x	x	√	√	√	√	√
BC-16	x	√	√	√	√	√	x	x	√
BC-17	x	√	√	√	√	x	x	x	x
BC-18	x	√	√	√	√	√	√	√	√

BC-2 and BC-19 were excluded from all analysis

Table 3. Permutation Importance (PI) calculated from Maxent analysis for bioclimatic environmental variables over three climatic time periods

Bio-climatic variables	Current (PI)	2050 RCPs				2070 RCPs			
		2.6	4.5	6	8.5	2.6	4.5	6	8.5
BC-1	-	15.1	-	-	-	-	-	-	-
BC-3	-	-	31.3	35.5	29.9	40.3	38.8	30.5	31.5
BC-4	-	37.7	-	-	-	-	-	-	-
BC-5	21.9	-	10.8	5.9	3.9	-	12.9	-	7.5
BC-6	6.6	-	13.6	40.7	35.9	10.9	-	3.8	-
BC-7	8.1	9.4	-	-	-	14.3	23.8	-	-
BC-8	-	4.8	4.5	1.5	0.6	3	1	3.6	-
BC-9	-	-	2.2	1.9	1.7	6.1	-	4.7	-
BC-10	-	-	-	-	6	-	-	11.6	-
BC-11	16.8	-	-	-	-	-	-	24	-
BC-12	30.9	25.7	33	-	-	-	-	-	-
BC-13	7.1	-	-	-	-	-	18	17.9	-
BC-14	-	0.2	0.4	0.4	-	1.1	-	0.2	6.8
BC-15	8.7	-	-	-	1.6	4	4.4	2.3	4.7
BC-16	-	4.6	2.2	12.2	0.8	19	-	-	35.9
BC-17	-	1.1	1.6	0.4	18.3	-	-	-	-
BC-18		1.3	0.4	1.5	1.4	1.3	1.1	1.4	13.6

35.9% PI were identified as the most influential predictors with RCPs of 2.6 and 8.5 in 2050 and 2070, respectively. Most RCPs found Precipitation of Driest Month (BC-14) as the least effective factor, followed by Precipitation of Warmest Quarter (BC-18). Among the non-climatic variables, ecosystem rooting depth (85.8%) and soil organic carbon (PI 74.5%) were identified as the most important and influential parameters for this species (Table 4).

Model performance: The area under the receiver operating curve (AUC) was used to evaluate the Maxent model's performance for predicting distribution of this species. The machine learning method performs excellently (AUC = 0.94) with the current bio-climatic timeframe (Fig. 3), but it performs poorly (AUC = 0.78) with ecosystem rooting depth and rooting zone water storage capacity and was good (AUC > 0.80) with surface soil attributes (Fig. 3). The present model's quality was high, with AUC values more than 0.90 for two future bio-climatic timeframes and four greenhouse gas scenarios. Figure 4 depicts the Jackknife test results with multiple predictors. These horizontal lines showed the variables with

Table 4. Permutation Importance (PI) calculated from Maxent analysis for non-bioclimatic environmental variables

Predictors	Permutation values
Ecosystem rooting depth	85.8
Rooting zone water storage size	14.2
Surface soil properties	
Soil organic carbon	74.5
Sand	6
pH	8.1
Soil bulk density	7.4
Clay contents	4

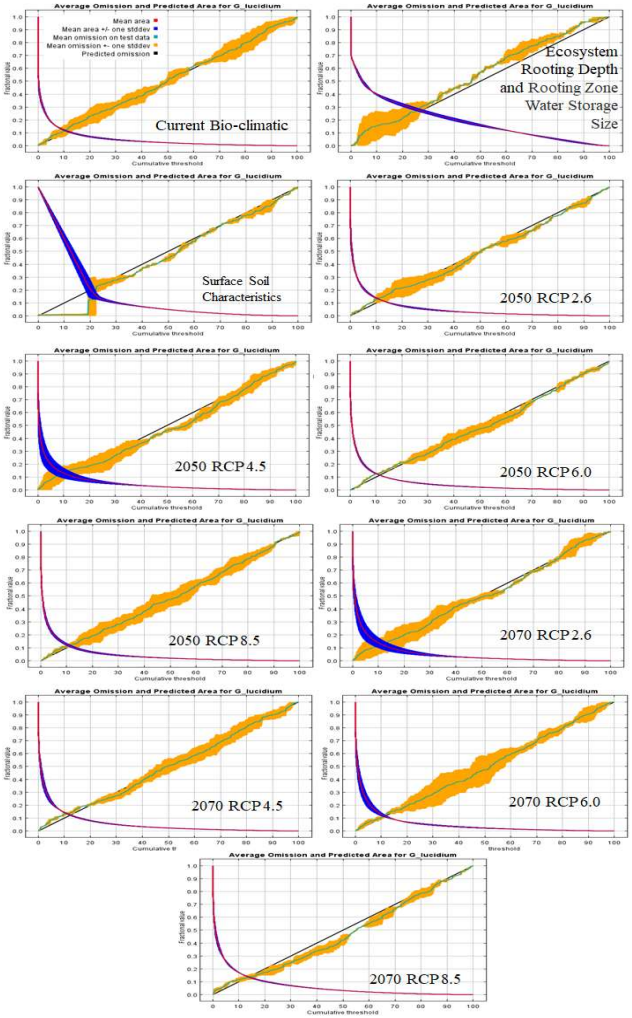

Fig. 2. Analysis of omission/commission with various bio-climatic timeframes and RCPs projection and non-climatic variables

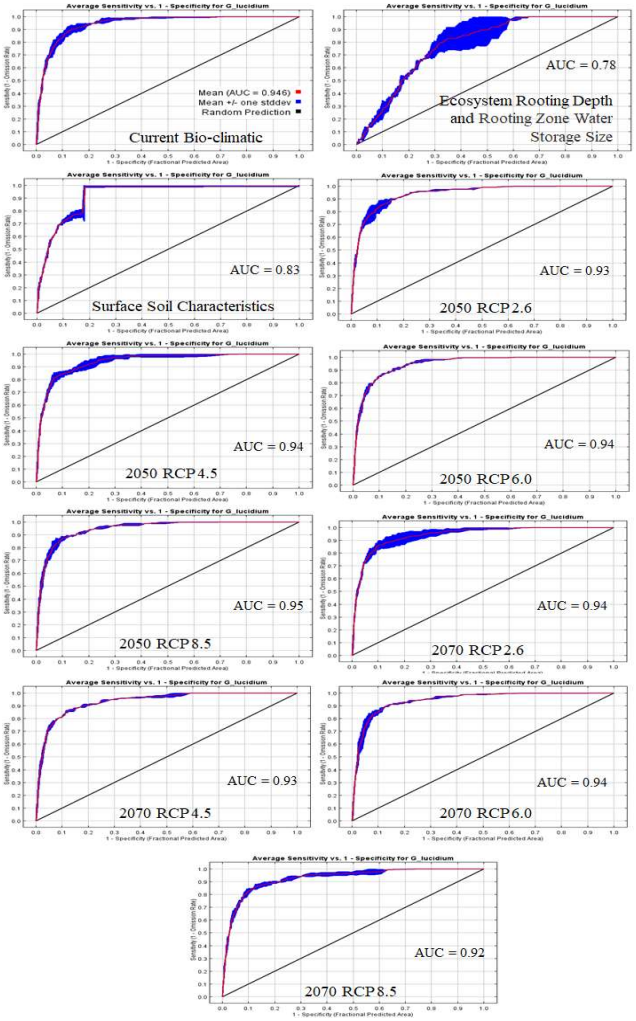

Fig. 3. Receiver Operating Characteristic (ROC) curves: with various bio-climatic timeframes and RCPs projection and non-climatic variables

the greatest gain when used alone, and hence appear to have the most significant information on their own (such variables can be referred as category 1 variables). The variables that reduce the gain the most when eliminated, and so appear to contain the most information that other variables do not category 2 variables. This study unearthed that the bio-climatic variables like mean temperature of coldest quarter (BC-11) functioned as category-1 variables for the current and 2070 RCP 6.0 time-frames, whereas the variables Maximum Temperature of Warmest Month (BC-5) and Isothermality (BC-3) functioned as category-2 variables for the same time-frames. In the 2050 RCP 2.6 and 2070 RCP 4.5 climatic projections, characteristics such as mean temperature of wettest quarter (BC-8) and isothermality (BC-3) were designated as category-1 variables. The identical catogry-1 (minimum temperature of coldest month: BC-6) and catogry-2 (Isothermality) characteristics that influenced the occurrence of this species during their respective climatic and RCP projections will exist during 2050 climatic timeframes (RCP 4.5, 6.0, and 8.5). RCP 8.5 of 2070 and non-climatic variables such as ESRD and WS, as well as soil properties, have category 1 and category 2 variables that are similar.

Trends of habitat suitability with respect to various significant category-1 predictors: The occurrence frequency of *G. lucidium* fluctuates as a function of major climatic, rooting depth, root zone water storage capacity, and surface soil variables depicted in Figure 5. The habitat suitability was higher toward the mean temperature of the coldest quarter (BC-11), and the maximum of habitat suitability with this predictor remained at temperatures -10 to $+10^0$ C for current climatic conditions (Fig. 5a) and -10 to 5^0C at 2070 RCP 6.0 (Fig. 5h). Minimum temperature of coldest month (BC-6) was best suited for this species with a range of -10 to $+10^0$ C with RCP 4.5 of 2050 (Figure 5c) and -10 to $+8^0$ C with RCP 4.5 (Figure 5d) and 6.0 (Fig. 5e) of the same time-frame. While its habitat was altered by Isothermality at a range of 20 to 40% during 2070 RCP 4.5 (Figure 5h) and 8.5 (Figure 5i), its suitability fell dramatically after these threshold values. Interestingly, during the RCP 2.6-time frame of 2050 and 2070, the mean temperature of the wettest quarter (BC-8 Fig. 5b) and the mean temperature of the driest quarter (BC-9 Figure 5f) were shown to be more beneficial for this species. However, their peak widths differed, 2050 peak width was recorded as being more border than 2070 peak width. With characteristics such as ecosystem rooting depth, this species' habitat preferentiality was continuously synchronised and reached a maximum of 8 cm before drastically decreasing (Fig. 5j). Similarly, soil organic carbon up to 145 (g/kg) was determined as most beneficial to this fungus's habitat suitability (Fig. 5k).

Spatial delineation of range contraction or expansion: Table 5 displays the spatial extent (in square kilometres) of various habitat types based on climatic (present and future estimates) and non-climatic variables. The largest area under the optimum habitat class (2983977.56 sq. km.) was recorded with current bio-climatic time-frame, while the lowest area (600355.52 sq. km) under this class was recorded with 2050 RCP 6.0. Similarly, maximum area under moderate (41829161.24 sq. km) and marginal (43356903 sq. km) habitat classes were recorded with ecosystem rooting depth and rooting zone water storage size. However, minimum areas under these classes were recorded with 2050 RCP 8.5 and surface soil properties, respectively. The later variables (soil) can support only its lower habitat type covering 108528601.18 sq. km area. Overall, under all classes, maximum total area (115217353.3 sq. km) was

Table 5. Area (sq km) of different habitat suitability classes with different climatic and non-bioclimatic predictors

Predictors	Area (Sq. Km.) under habitat suitability classes				
	Optimum	Moderate	Marginal	Lower	Total
Current BC	2983977.56	8735251.80	13418953.33	34299321.62	59437504.32
Surface soil properties	2098660.69	2080085.48	2050899.83	108528601.2	114758247.2
Root and water	2926892.06	41829161.24	43356903	27104397	115217353.3
2050 RCP 2.6	1735993.21	4280904.28	4280904.28	13527374.83	23825176.6
2050 RCP 4.5	969631.30	1910274.91	4588175.75	11671040.62	19139122.59
2050 RCP 6.0	600355.52	1721083.65	4334096.50	10743475.03	17399010.71
2050 RCP 8.5	674798.4962	1346748.766	3714953.407	9700582.672	15437083.34
2070 RCP 2.6	640858.7371	1645626.473	3840950	14072832.65	20200267.86
2070 RCP 4.5	829087.6135	1656671.308	3900602.178	15210570.79	21596931.89
2070 RCP 6.0	678794.6695	1657296.388	4375988.385	9631468.338	16343547.78
2070 RCP 8.5	1070867.593	3333235.379	8576820.252	16455387.61	29436310.83

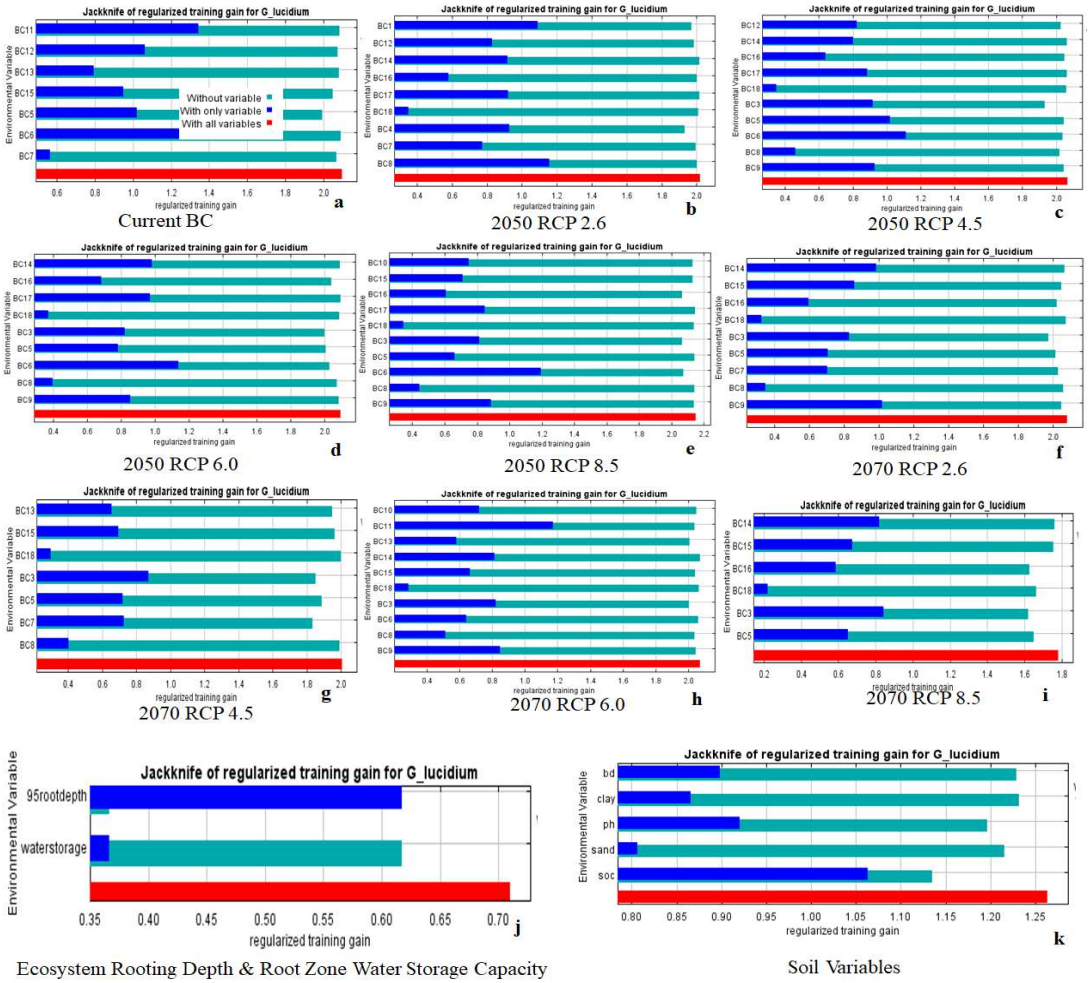

Fig. 4. Jackknife test of training data set to identified of variables with maximum gain and loss in model qualities

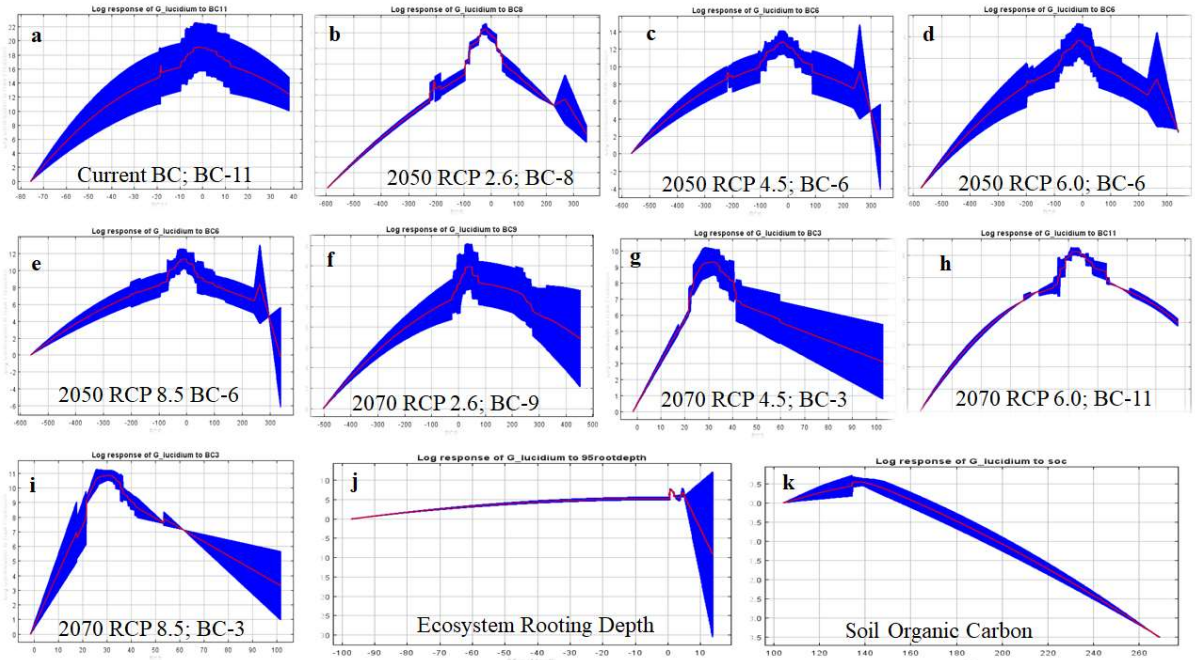

Fig. 5. Response curves with various climatic and non-climatic parameters illustrating the likelihood of *G. lucidum* habitat suitability

recorded with rooting variables, while the overall lowest area under all classes (15437083.34 sq. km.) was recorded with 2050 RCP 8.5. Further, percent changes for the area under different habitat classes (through climatic variables only) with respect to current areas under these classes. Our analysis suggested that optimum habitat class for *G. lucidum* will be reduced by - 41.82 (2050 RCP 2.6) to -79.88 (2050 RCP 6.0 Table 6) compared to its current area. Similarly, moderate area reduced from -50.99 (2050 RCP 2.6) to -84.58 (2050 RCP 8.5). Such trends were also recorded for marginal and low habitat types also. Such result indicates that this species will lose its area under all types of habitats with studied climatic and non-climatic predictors.

Spatial extent of optimum class: KML analysis of the ASCII file of the maxent output suggested that the optimum areas within current climatic conditions are located in southern India, including Karnataka (Tilvalli, Anavatti, Hosakawali, Hebri, Varanga, Bramavara, Belve, Thenka Bettu, and Kundapura), Maharashtra (Tilvalli, Anavatti, Hosakawali, Hebri, Varanga, Bramavara (particularly Ratnagiri, Kolhapur, Goa, Belagavi, Pune and Mumbai). Various marginal areas can also be found in western portions of the country, such as Gujarat (Tharad, Bhuj, Somnath, Porbandar, Bhanvad), Rajasthan (Sanchor, Bhinmal, Jalore, Pali, Malpura, Jhalawar, Guna), and some districts of Uttar Pradesh and Madhya Pradesh (Fig. 6). The greatest region is classified as optimal, and it includes primarily European countries such as the United Kingdom, Denmark, the Netherlands, Poland, territories next to the Baltic Sea, and patches in Germany and Switzerland. It can see from Google Earth that these countries provided optimal to moderate conditions for this fungus (Fig. 7). Current non-climatic characteristics, such as ecosystem rooting depth and root zone water storage capacity, revealed increasingly dispersed optimum categories around the world, including India, China, Zimbabwe, the Democratic Republic of the Congo, Hungary, Brazil, and some states in the United States (Figure 6 and 7). The surface soil parameters indicated that there was greater land under marginal and low suitability for this fungus. Using these non-climatic characteristics, optimal regions were identified in Belarus, Poland, Norway, Sweden, Finland, Chhattisgarh, sections of Maharashtra (Nagpur, Pune), and several states in the United States of America.

With a predicted climatic time-frame of 2050 and RCP 2.6, there will be a decline in optimum areas from Indian continents (Fig. 8), and this fungus will be found in isolated spots in southern India. Our findings also demonstrated a significant decline of this fungus in the European region, which will be predominantly exhibited in Denmark (Fig. 9). However, with RCP 4.5 and a similar climatic time frame, a somewhat larger area under the optimal class, notably covering Italy and parts of Georgia. Furthermore, the least area under this class will occur if RCP 6.0 (2050) operates, and within India, few isolated patches will occur only in the south, while the largest area under this class will remain in Denmark and neighbouring areas. In terms of the area under the optimum class, if RCP 8.5 is implemented (2050), a similar situation will be maintained, and our analysis suggests that isolated optimal areas in India's southern and western parts will be transformed to low suitable areas. However, a new optimal class area would arise in the country's eastern section, Meghalaya. Similarly, the highest area in this category will stay in Denmark, with no increase in size in the Denmark parts toward Sweden (Fig. 9). With 2070 RCP 2.6, the optimum area will fall drastically in comparison to current climatic conditions (Fig. 10), and within India, just a few isolated patches (Maharashtra and Karnataka) and two patches at Rajasthan will be detected (one new Mount Abu and one near Ajmer district). Our examination of European countries clearly shows that the majority of the optimum areas in Belgium, the Netherlands, and the United Kingdom will be converted to the moderate category (Fig. 11). A large patch of low habitat suitability will be detected in China during this GHG period. However, there will be a rise in area under

Table 6. Per cent changes under four studied habitat suitability classes with two bio-climatic timeframes and four RCPs with respect to current bioclimatic conditions

Bio-climatic time frames and RCPs	Optimum	Moderate	Marginal	Low
2050 RCP 2.6	-41.82	-50.99	-68.10	-60.56
2050 RCP 4.5	-67.51	-78.13	-65.81	-65.97
2050 RCP 6.0	-79.88	-80.30	-67.70	-68.68
2050 RCP 8.5	-77.39	-84.58	-72.32	-71.72
2070 RCP 2.6	-78.52	-81.16	-71.38	-58.97
2070 RCP 4.5	-72.22	-81.03	-70.93	-3.63
2070 RCP 6.0	-77.25	-81.03	-67.39	-71.92
2070 RCP 8.5	-64.11	-61.84	-36.08	-52.02

the optimal class with RCP 4.5 (2070) in compared to RCP 2.6, which will be present in the United Kingdom (Manchester, Birmingham, Bristol), Netherlands and Belgium areas toward the Northern Sea. Within India, the optimal class will occur exclusively in the southern region, mainly Maharashtra, whereas Rajasthan parts will be

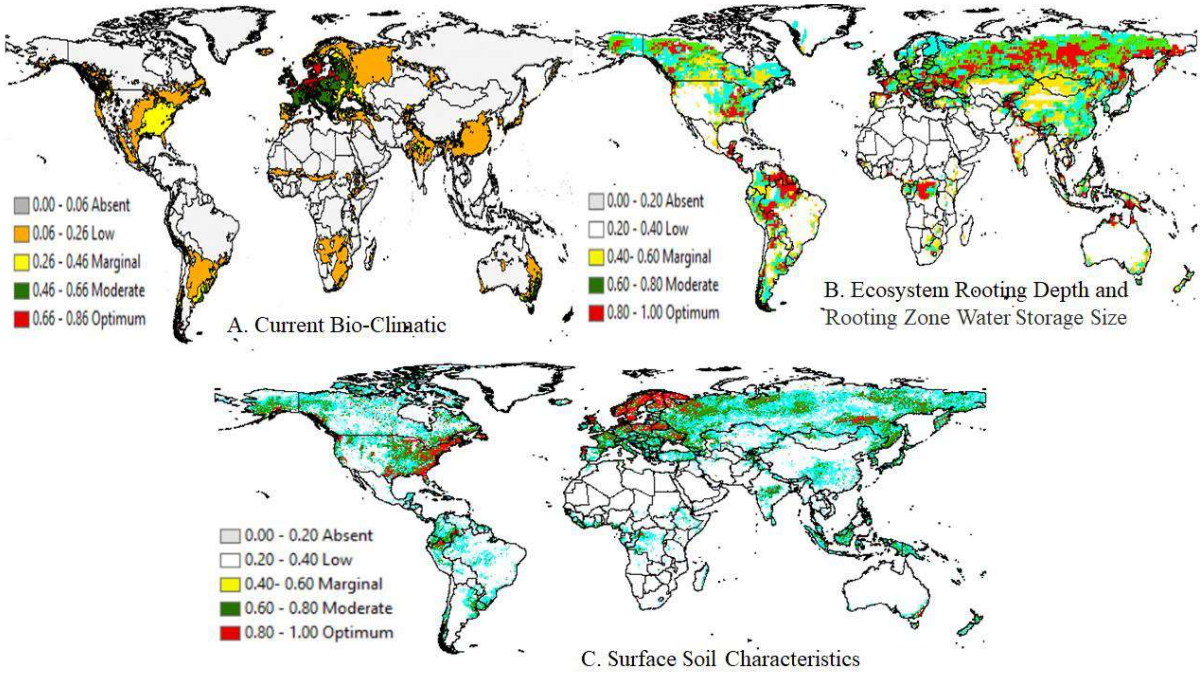

Fig. 6. Habitat suitability classification of *G. lucidum* with current bio-climate, surface soil, ecosystem rooting depth (95%), total plant-available water storage capacity of the rooting zone (TPAWSC RZ) predictors

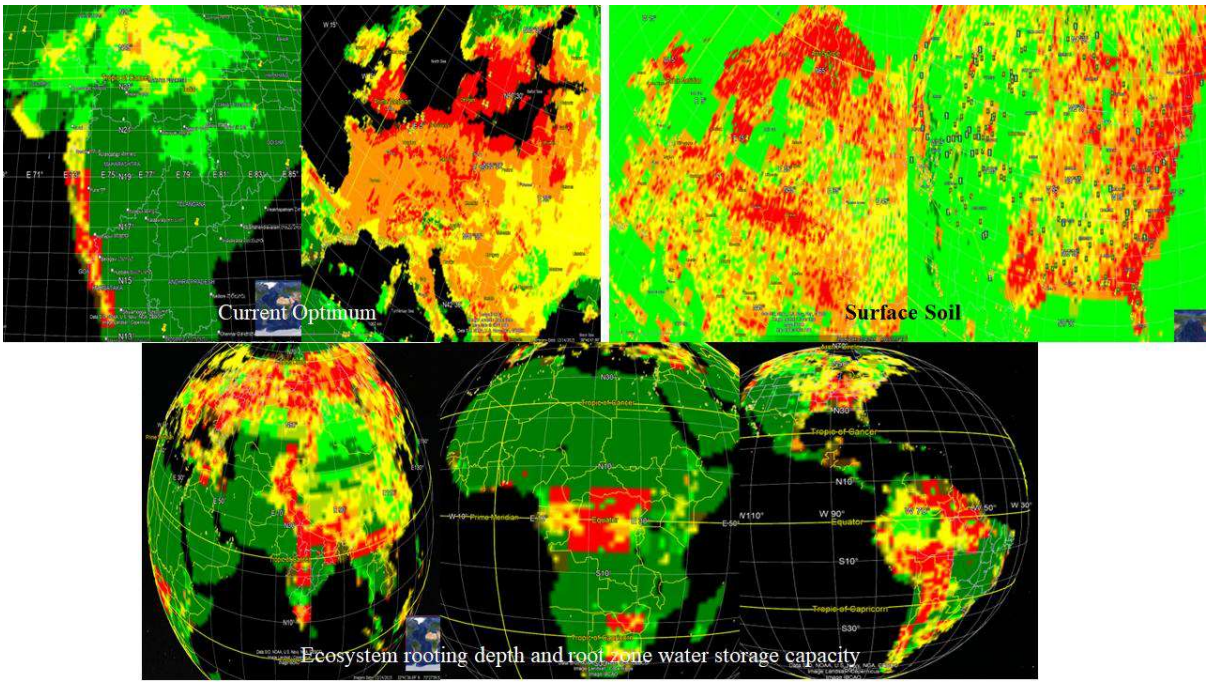

Fig. 7. Spatial distribution of *G. lucidum* captured with conversion of Maxent output to KML file showing impacts of current bio-climatic, surface soil properties and ecosystem rooting depth (95%) and total plant-available water storage capacity of the rooting zone predictors

unsuitable. With RCP 6.0 (2070), there will be a significant drop in optimum habitat in the European region, with only Denmark and a few places in the Netherlands and Belgium remaining. Except for a patch in Meghalaya, no such class will exist within the Indian subcontinent. Surprisingly, a larger area under the optimal category with RCP 8.5 (2070) than

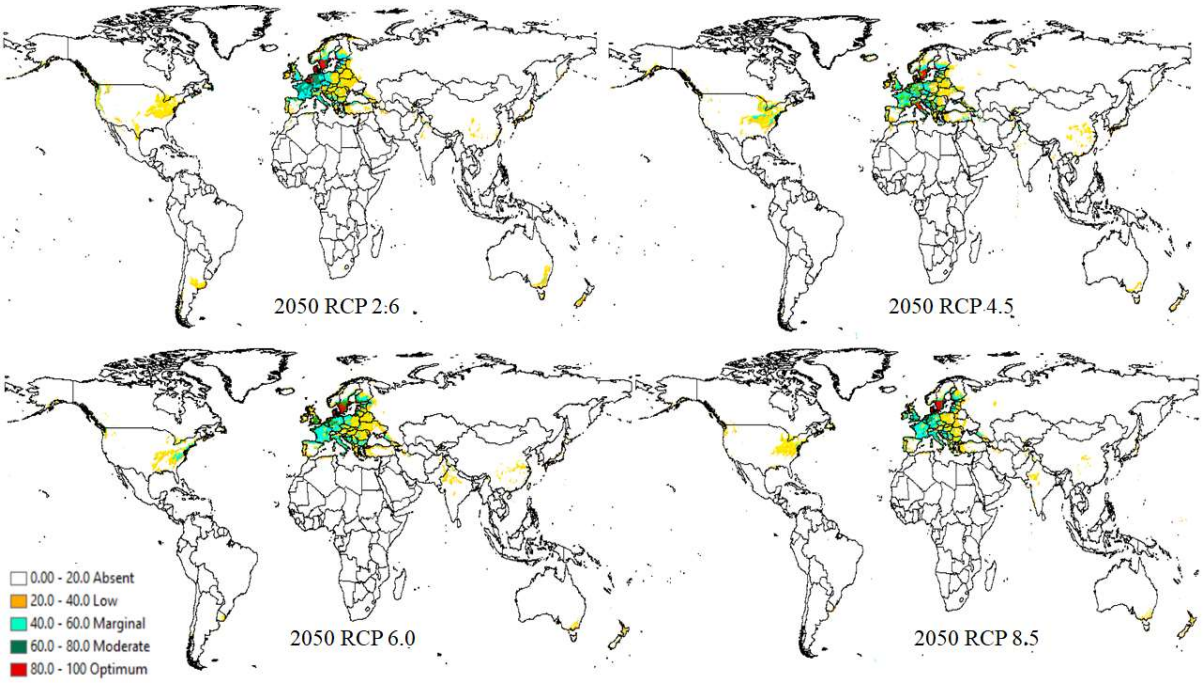

Fig. 8. Habitat suitability classification of *G. lucidum* with 2050 bio-climatic timeframes along with four RCPs viz. 2.6, 4.5, 6.0 and 8.5

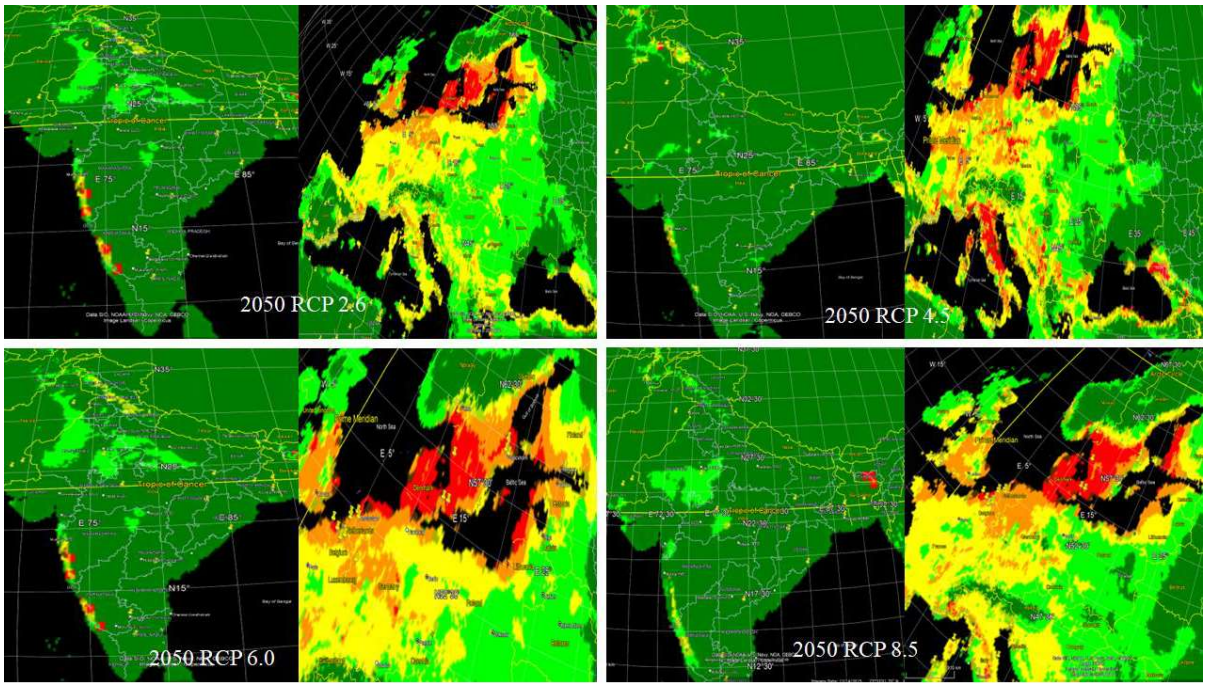

Fig. 9. Spatial distribution of *G. lucidum* captured with conversion of Maxent output to KML file showing impacts of 2050 bio-climatic variables along with four RCPs viz. 2.6, 4.5, 6.0 and 8.5

with the previous three RCPs. With this RCP, the southern coast of Maharashtra (Fig. 11) and, to a lesser extent, the eastern section of Meghalaya will be the focal point for this species. Afghanistan and Tajikistan will also have isolated portions of optimal class. Denmark and parts of the United Kingdom will be the most suitable European country for this fungus. While parts in the Netherlands, Belgium, and France will be classified as moderately suitable.

Plant fungi have a diverse geographical range and can thrive in tropical, subtropical, and temperate countries (Baino

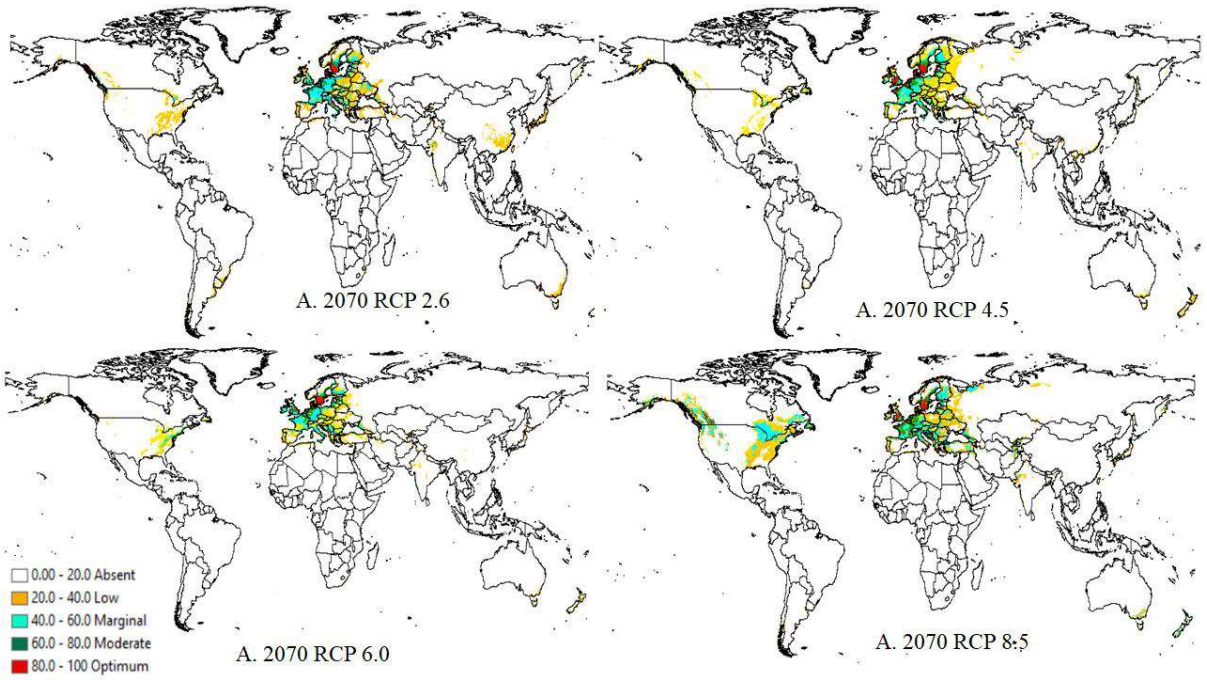

Fig. 10. Habitat suitability classification of *G. lucidum* 2070 bio-climatic timeframes along with four RCPs viz. 2.6, 4.5, 6.0 and 8.5

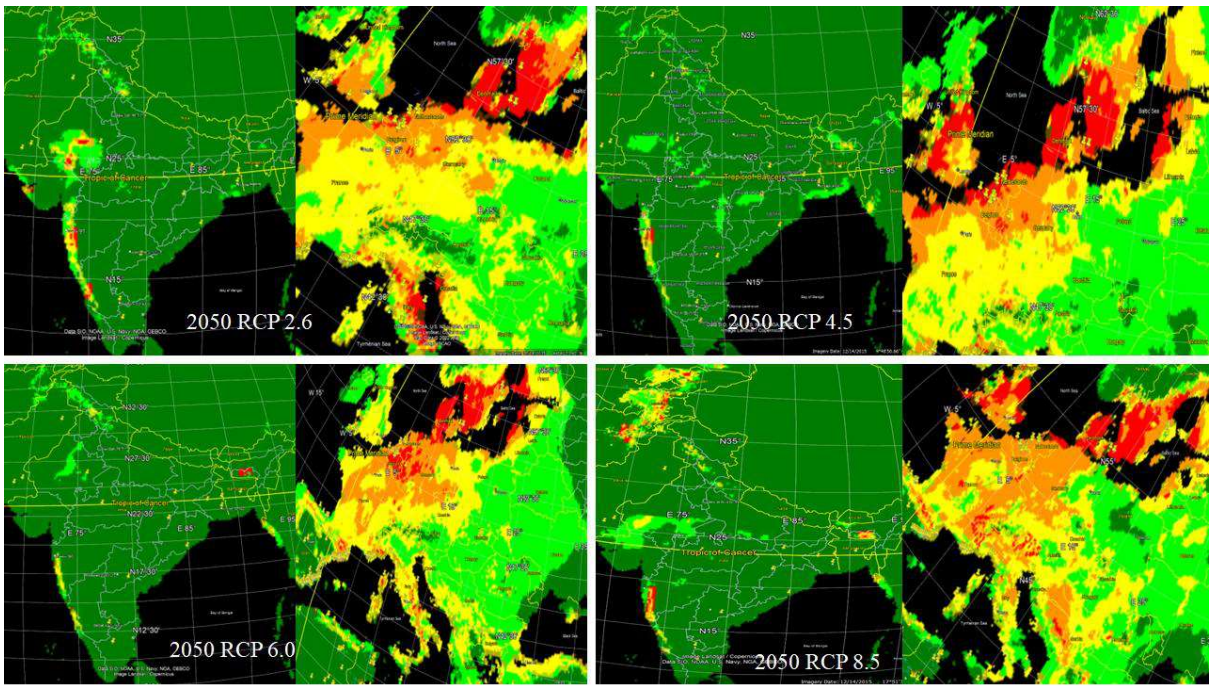

Fig. 11. Spatial distribution of *G. lucidum* captured with conversion of Maxent output to KML file showing impacts of 2070 bio-climatic variables along with four RCPs viz. 2.6, 4.5, 6.0 and 8.5

et al 2011, Cohen et al 2022). However, their eco-climatic niche modelling is comparatively lesser than the plants and animals that may be linked with requisition of deep ecological understanding for such analysis (Ireland and Kiritcos, 2019). Species distribution modelling (SDM) refers to statistical methodologies for determining a species' potential geographical spread and ecological needs (Mathur and Sundaramorthy et al. 2019). The mathematical output of SDM can be either an equation that ties the expected distribution of a species to a collection of environmental predictors or a response curve that describes how the predictors affect species distribution. SDM has been used in a variety of areas, including global change biology, biogeography, and conservation management (Li et al 2020). With presence-absence data SDM, involves two different sub-groups i.e., regression based and machine learning. Use of Maxent tool for plant fungi distribution assessment were carried out on *Polyporus umbellastus* (Liu et al 2015, Guo et al 2019), *Ganoderma lucidum* (Copot and Tanase 2017), *Suillus lakei* (Pietras et al 2018), *Tricholoma matsutake* (Guo et al 2017), *Fomitopsis pinicola*, *Porodaedalea laricis*, *Piptoporus betulinus* and *Trametes* suaveolens (Yuan et al 2019), *Calthrus archeri* (Birsan et al 2021), *Agaricus campestris, Calocybe gambos, Helvella crispa, Hypholoma lateritium, Mycena polygramma, Panaeolus foenisecii, Ramaria gracilis, Mycena polygramma* and *Mycena polygramma* (Stojek et al 2022), *Arcyria cinerea*, *Perichaena depressa* and *Hemitrichia serpula.*

A number of studies have demonstrated the utility of species distribution modelling (SDM)/or ecological niche modelling (ENM) for plant fungi in a variety of scientific inventories, including those concerned with estimating the likelihood of disease spread (Watt et al 2011, Yonow et al 2013), quantifying the value of assets (plant hosts) vulnerable to the pathogen (Watt et al 2009), and estimating costs (Chakraborty et al 1998, Ganley et al 2011, Yonow et al 2013). SDM could be an interdisciplinary plant fungal activity that has a favourable impact on global and regional policy responses. In recent years, the use of fungal SDM (F-SDM) has increased considerably in a variety of industries. F-SDMs were created for a variety of reasons, and according to Hao et al (2020) majority of them can be put into three broad categories (1) investigating environmental covariates of occurrence, (2) predicting occurrence in areas of interest, and (3) using fungi as a model organism to study methodological or ecological theories. In the current study, strong predictive model capabilities using bio-climatic time-frames and their related RCPs (AUC > 0.9) when compared to top-down variables such as soil parameters, ecosystem rooting depth, and root zone water holding capacity. As a result, it may conclude that bio-climatic variables will be the primary controlling elements affecting the habitat appropriateness of this fungus globally. Our findings also demonstrated a constant deterioration in *G. lucidium* optimum habitat with all forecasted RCPs and non-bioclimatic factors when compared to existing bio-climatic circumstances. Such findings are consistent with those of Vetrovsky et al (2019), demonstrated that several environmental conditions influence the global distribution of fungi, with climate being the most influential for the most common fungal species. The relative importance of mean driest quarter temperature (BC-9), precipitation seasonality, and fungal taxa distribution in decreasing order (BC-15), wettest quarter temperature (BC-8), coldest quarter precipitation (BC-19), mean diurnal range (BC-2), gross primary production, bulk density, and pH were all reported. Threshold limits for various secondary parameters were also identified, such as ecosystem rooting depth and soil organic carbon.

Plant fungal communities (dominated by Leotiomycetes, Agaricomycetes, Eurotiomycetes, and Sordariomycetes) are influenced by abiotic environmental variables such as soil (pH, nutrients, and particle size distribution) and climate (mean annual temperature and mean annual precipitation, Mathur, 2014b, Van Geel et al 2018; Wu et al 2018). Such bottom-up and top-down predictive variables also have temporal effects. For example, in two Japanese mountain habitats, temperature changes were identified to be the principal driver of variance in fungal community composition (Miyamoto et al 2015), but in Europe, AM fungal community composition was most substantially controlled by soil features (Van Geel et al 2018). Similarly, Vetrovsky et al (2019) used Random Forest analysis to assess the Variable Importance (VI) for the global distribution of 457 fungal species, and the VI were in the following order: wettest quarter mean temperature (BIO8)> coldest quarter precipitation (BIO 19)> diurnal temperature range (BIO2)> gross primary production> warmest quarter precipitation (BIO8).

In this study, it was observed that energy-related bio-climatic variables (BC-1 to BC-11, Table 3) had the greatest impact on the habitat types of this fungus, while precipitation-related variables (BC-12 to BC-19) have a lesser impact. Wang et al. (2018) used the same modelling approaches to anticipate future distribution *Pseudomonas syringae* pv. *actinidiae* (Psa) in China. Their research found that the highest April temperature (19%), the coldest quarter mean temperature (41%), and the lowest October temperature (10.8%) had the greatest influence on Psa spread. Furthermore, as temperature and moisture stress increase,

M. phaseolina dry root rot and charcoal rot become more severe. Temperature increases (35-40°C) create pathogenic microsclerotia, exposing hosts to infection (Olaya and Abawi, 1996). High temperatures and dry conditions promote the growth of microsclerotia and increase the activity of hydrolytic enzymes within the microsclerotia, making infection simpler (Lalita and Ahir, 2020). Rising temperatures are expected to have an impact on the geographical distribution, virulence pattern, and presence of *M. phaseolina* in new areas in the near future (Arias et al 2011).

According to previous studies, *G. lucidum* mycelial growth is temperature-dependent, and this environmental factor essentially makes it easier for bacteria to grow on the fungus' fruiting body. By affecting the polysaccharide and other microelements in *G. lucidum* fruiting bodies through their enzymatic action, such bacteria support the growth of this fungus (Stajic et al 2002, Tanaka et al 2016). Jayasinghe et al (2008) have concluded that minimum and maximum cardinal temperatures for the mycelial growth and density of *G. lucidum* were 15 and 35° C, respectively. The best mycelial growth was reported between 30° C to 35° C. However, the current study suggested that with different RCPs and climatic time frames, habitat niche of this species will respond more toward the mean temperature of the coldest quarter (BC-11), and the maximum of habitat suitability with this predictor remained at temperatures -10 to $+10^0$ C for current climatic conditions (Fig. 5a) and -10 to 5^0C at 2070 RCP 6.0 (Fig. 5h). Minimum temperature of coldest month (BC-6) was best suited for this species with a range of -10 to $+10^0$ C with RCP 4.5 of 2050 (Fig. 9c) and -10 to $+8^0$C with RCP 4.5 (Fig. 5d) and 6.0 (Fig. 5e) of the same time-frame. While its habitat was altered by Isothermality at a range of 20 to 40% during 2070 RCP 4.5 (Fig. 5h) and 8.5 (Fig. 5i), its suitability fell dramatically after these threshold values. Thus, our study clearly demonstrates the decrease breadth of atmospheric temperature variabilities for this fungus.

Isothermality, which is a measure of how large day-to-night temperature oscillations are relative to the summer-to-winter (annual) oscillations, was found to be the most important factor for this species under the majority of climatic time-frame and greenhouse gas scenarios. An isothermal value of 100 indicates that the diurnal temperature range is comparable to the annual temperature range, whereas anything less than 100 (~30) indicates that the temperature variability is greater during an average month than it is throughout the entire year. In this study, lower isothermality values, indicating that seasonal variations may have a greater effect on the dispersal of this fungus than monthly temperature fluctuations.

It was also noticed that ecosystem rooting depth and rootzone water storage capabilities are pre-disposing factors for *G. lucidium* in the current environment. This is supported by the findings of Bhansali (2012), Ren et al (2020), and Fatmia et al (2022). Further lesions on the root surface promote fungal penetration into the host vascular system. However, no information about the rooting depth threshold that best supports this fungus's habitat was previously accessible. Based on the output of Response Curve Function (ROC), it can be depict the establishment mechanism of this fungus as it relates to optimal root depth and moisture availability. According to the analysis, 8 cm depth is the most optimum for this fungus growth, and anything beyond that reduces the fungus's habitat suitability dramatically. Furthermore, its well known that this fungus infection spreads directly from root to root, implying the importance of root lengths.

The spatial breadth of this fungus was also studied, and such field-based prediction can be utilised to estimate its wild region-specific production output, which can also be synchronised with its in-vitro propagation to fulfil industrial demands. Europe, for example, has the most potential for this species, followed by a few states in the United States. For improved assessments in Asian, African, and Australian locations, field-based exploration in remote/wild places is required. Despite the fact that many pharmacological clinical trials from China have been documented, as well as the pathogenic nature of this fungi on *Prosopis cineraria* tree and oil palm plantation from Indian regions, a lack of systematic surveys with proper geo-graphical coordinates impedes habitat-based niche modelling with advanced Machine Learning tools from such areas.

CONCLUSION

The machine learning Maxent modelling technique achieved outstanding model characteristics for *Ganoderma lucidum* fungus (AUC 0.90). Bioclimatic-energy variables (temperature) will more effectively manage its future global dispersion than water considerations (precipitation). In compared to the current optimum and moderate habitat areas, our research found a significant decline with examined predictors ranging from -73.74 to -87.56. This fungus, might assume, is constantly spreading over some European countries. However, within Asian regions, both optimum and moderate habitat suitability for this species will deteriorate, making wild collection for diverse pharmaceutical product manufacture more difficult. As a result, its availability in such locations will be heavily reliant on its *in-vitro* conditions (substratum) as well as the adjustment of micro-environmental variables identified in this work.

CONTRIBUTION

Senior author conceptualized the chapter theme and interpretation of output of various machine learning techniques. Co-Author prepared various types of language codes in python, Java and in R scripts and convert the various file format from ASCII to KML, Raster, dbf, CSV etc for software's like QGIS 3.10.0, Wallace, DIVA-GIS version 7.5, MaxEnt 3.4.1 software, SDM toolbox, Map Comparison Kit, ENMTools and Ntbox, SSDM R packages.

REFERENCES

Alam N, Lee J and Lee T 2010. Mycelial growth conditions and phylogenetic relationships of *Pleurotus ostreatus. World Applied Science Journal* **9**(8): 928-937.

Arias RS, Ray JD, Mengistu A and Scheffler BE 2011. Discriminating microsatellites from *Macrophomina phaseolina* and their potential association to biological functions. *Plant Pathology* **60**: 709-718.

Baino OM, Salazar SM, Ramallo AC and Kirschbaum DS 2011. First report of *Macrophomina phaseolina* causing strawberry crown and root rot in north-western Argentina. *Plant Disease* **95**(11): 1477.

Basnet BB, Liu L, Bao L and Liu H 2017. Current and future perspective on antimicrobial and anti-parasitic activities of Ganoderma sp.: An update. *Mycology* **8**: 111-124.

Bhansali RR 2012. Ganoderma disease of woody plants of Indian arid zone and their biological control. In: *Plant Defence: Biological Control, Progress in Biological Control*. Merillon JM and Ramawat KG (Eds). Springer Science. DOI 10.1007/978-94-007-1933-0_9, 209-238.

Bhansali RR 2012. Ganoderma disease of woody plants of Indian arid zone and their biological control. In: *Plant Defence: Biological Control, Progress in Biological Control*. Merillon JM and Ramawat KG (Eds). Springer Science. DOI 10.1007/978-94-007-1933-0_9, 209-238.

Bijalwan A, Bahuguna K, Vasishth A, Singh A, Chaudhary S, Dongariyal A, Thakur TK, Kaushik S, Ansari MJ, Alfarraj S, Alharbi SA, Skalicky M, Brestic M 2021. Growth performance of *Gandoerma lucidum* using billet method in Garhwal Himalaya India. *Saudi Journal of Biological Sciences* **28**: 2709-2717.

Bijalwan A, Vasishth A, Singh A, Chaudhary S, Tyagi A, Thakur MP, Thakur TK, Dobriyal M, Kaushal R, Singh A, Maithani N, Kumar D, Kothari G and Chourasia PK 2020. Insights of medicinal mushroom (*Ganoderma lucidum*): Prospects and potential in India. *Biodiversity International Journal* **4**(5): 202-209.

Birsan C, Mardari C, Copot O and Tanase C. 2021. Modelling the potential distribution and habitat suitability of the alien fungus *Calthrus archeri* in Romania. *Botanica Serbica* **45**(2): 241-250.

Cao Y, Wu SH and Dai YC 2012. Species clarification of the prize medicinal Ganoderma mushroom "Lingzhi". *Fungal Diversity* **56**(1): 49-62.

Chakraborty S, Murray GM, Magarey PA, Yonow T, Sivasithamparam K, O'Brien RG, Croft BJ, Barbetti MJ, Old KM, Dudzinski MJ, Sutherst RW, Penrose LJ, Archer C and Emmett RW 1998. Potential impact of climate change on plant diseases of economic significance to Australia. *Australasian Plant Pathology* **27**(1): 15-35.

Chan SW, Brian T, Paul C and Christopher WKL 2021. The beneficial effects of *Ganoderma-lucidum* on cardiovascular and metabolic disease risk. *Pharmaceutical Biology* **59**: 1159-1169.

Coban HO, Orucu OK, Arslan ES 2020. MaxEnt modelling for predicting the current and future potential geographical distribution of *Quercus libani* Olivier. *Sustainability* 2671. doi:10.3390/su12072671

Cohen R, Elkabetz M, Paris HS, Gur A, Dai N, Rabinovitz O and Freeman S 2022. Occurrence of *Macrophomina phaseolina* in Israel: Challenges for disease management and crop germplasm enhancement. *Plant Disease* **106**: 15-25.

Copot V and Tanase C 2017. MAXENT modelling of the potential distribution of *Ganoderma lucidum* in North -Eastern region of Romania. *Journal of Plant Development* **24**: 133-143.

Cotrina Sánchez A, Rojas Briceño NB, Bandopadhyay S, Ghosh S, Torres Guzmán C, Oliva M, Guzman BK and Salas López R 2021. Biogeographic distribution of *Cedrela* spp. genus in Peru using MaxEnt Modelling: A Conservation and Restoration Approach. Diversity **13:** 261. https://doi.org/10.3390/d13060261

Dawit A 1998. *Mushroom Cultivation: A Practical Approach*. Birhannaselam Printing Enterprise, Addis Ababa

Djebbouri M, Yahiaoui FZ and Terras M. 2021. Predicting habitat suitability of *Pistacia atlantica* DESF with maxent and GIS in the north western region of Algeria. *Bio Nature* **41**(2): 13-23.

El Sheikha AF 2022. Nutritional profile and health benefits of Ganoderma lucidum "Lingzhi, Reishi, or Mannentake" as functional foods: Current scenario and future perspectives. *Foods* **11**: 1030.

Fatima S, Khan F, Asif M, Alotaibi SS, Islam K, Shariq M, Khan A, Ikram M, Ahmad F and Khan TA 2022. Root-knot disease suppression in eggplant based on three growth ages of *Ganoderma lucidum*. *Microorganisms* **10**: 1068. https://doi.org/10.3390/ microorganisms10051068

Flory AR, Kumar S, Stohlgren TJ, Cryan PM 2012. Environmental conditions associated with bat white nose syndrome mortality in the north-eastern United States. *Journal of Applied Ecology* **49**: 680-689.

Ganley RJ, Watt MS, Kriticos DJ, Hopkins AJM and Manning LK 2011. Increased risk of pitch canker to Australasia under climate change. *Australasian Plant Pathology* **40**(3): 228-237.

Guo Y, Li X, Wei H, Guo B and Gu W 2017. Prediction of the potential geographic distribution of the ectomycorrhizal mushroom *Tricholoma matsutake* under multiple climate change scenarios. *Scientific Reports* **7**: 46221 | DOI: 10.1038/srep46221

Guo Y, Li X, Zhao Z and Nawaz Z 2019. Predicating the impacts of climate change, soils and vegetation types on the geographic distribution of *Polyporus umbellatus* in China. *Science Total Environment* **648**: 1-11.

Hanley JA, McNeil BJ 1982. The meaning under a receiver characteristic and use of the area operating (ROC) curve. *Radiology* **143:** 29-36.

Hao T, Guillera-Arroita G, May TW, Lahoz-Monfort JJ and Elith J. 2020. Using species distribution models for fungi. *Fungal Biology Reviews* **34**(2): 74-88.

Hapuarachchi KK, Elkhateeb WA and Karunarathna SC 2018. Current status of global *Ganoderma* cultivation, products, industry and market. *Mycosphere* **9**(5): 1025-1052.

Hennicke F, Cheikh-Ali Z, Liebisch T, Macia-Vicente JG, Bode HB and Piepenbring M. 2016. Distinguishing commercially grown Ganoderma lucidum from *Ganoderma lingzhi* from Europe and East Asia on the basis of morphology, molecular phylogeny, and triterpenic acid profiles. *Phtyochemistry* **127**: 29-37.

Hijmans RJ, Guarino L, Cruz M and Rojas E 2001. Computer tools for spatial analysis of plant genetic resources data: 1. DIVA-GIS. *Plant Genet Resource and Newsletter* **127**: 15-19.

Hijmans RJ, Cameron SE, Parra JL, Jones PG and Jarvis A 2005. Very high-resolution in-terpolated climate surfaces for global land. *International Journal of Climatology* https://doi.org/10.1002/joc.1276

Hyde KD, Bahkali AH and Moslem MA 2010. Fungi: An unusual source for cosmetics. *Fungal Diversity* **43**: 1-9.

Ireland KB and Kiritcos DJ 2019. Why are plant pathogens under-represented in eco-climatic nice modelling? *International Journal of Pest Management*. https://doi.org/10.1080/09670874.2018.1543910

Jindal SK, Singh DV, Moharana PC and Patel N 2009. *Annual Report: ICAR-Central Arid Zone Research Institute,* Jodhpur, India. Pages 156.

Jindal SK, Singh DV, Moharana PC and Patel N 2010. *Annual Report: ICAR-Central Arid Zone Research Institute,* Jodhpur, India. Pages 174.

Kaky E and Gilbert F 2019. Assessment of the extinction risk of medicinal plants in Egypt under climate change by integrating species distribution models and IUCN Red List criteria. *Journal of Arid Environment* **170**: https://doi.org/10.1016/j.jaridenv .2019.05.016

Kass JM, Vilela B, Aiello-Lammens ME, Muscarella R, Merow C and Anderson RP. 2018. *Wallace*: A flexible platform for reproducible modeling of species niches and distributions built for community expansion. *Methods in Ecology and Evolution* **9**: 1151-1156.

Khara HS 1993. Incidence of Ganoderma lucidum root rot on some tree species around Ludhiana. *Plant Disease Research* **8**(2): 136-137.

Khara HS and Singh J 1997. Diagnosis of Ganoderma lucidum root rot of trees, the cultural characteristics, spore germination and percentage of root-decay. *Plant Disease Research* **12**(2): 108-112.

Kleidon A 2011. ISLSCP II Total Plant-Available Soil Water Storage Capacity of the Rooting Zone. In Hall, Forrest G., G. Collatz, B. Meeson, S. Los, E. Brown de Colstoun, and D. Landis (eds.). *ISLSCP Initiative II Collection*. Data set. Available on-line [http://daac.ornl.gov/] from Oak Ridge National Laboratory Distributed Active Archive Center, Oak Ridge, Tennessee, U.S.A. doi:10.3334/ORNLDAAC/1006

Kumar S and Stohlgren TJ 2009. MaxEnt modelling for predicting suitable habitat for threatened and endangered tree *Canacomyrica monticola* in New Caledonia. *Journal of Ecology and Natural Environment* **1:** 94-98.

Kumar S, Stohlgren TJ and Chong GW 2006. Spatial heterogeneity influences native and non-native plant species richness. *Ecology* **87**: 3186-3199.

Lalita L and Ahir RR 2020. *In-vivo* evaluation of different fungicides, plant extracts, biocontrol agents and organics amendments for management of dry root rot of chickpea caused by *Macrophomina phaseolina*. Legume Research **43**: 140-145.

Lee SS 1985. *Tree diseases and wood deterioration problems in Peninsular Malaysia*, Occasional Paper No. 5. Faculty of Forestry, Agriculture, University of Malaysia

Li S, Shakoor A, Wubet T, Zhang N, Liang Y and Ma K 2018. Fine-scale variations of fungal community in a heterogeneous grassland in Inner Mongolia: Effects of the plant community and edaphic parameters. *Soil Biology and Biochemistry* **122**: 104-110.

Li Y, Tang ZY, Yan YJ, Wang K, Cai L, He J, Song G and Yao YJ 2020. Incorporating species distribution model into the red list assessment and conservation of macro-fungi: A case study with *Ophiocordyceps sinensis*. *Biodiversity Science* **28**: 99-106.

Limbo-Dizon JE, Almadrones-Reyes KJ, Bacabago SAB and Dagamac NHA 2022. Bioclimatic modeling for the prediction of the suitable regional geographical distribution of the selected bright-spored Myxomycetes in Philippine archipelago. *Biodiversitas* **23**(5): 2285-2294.

Liu MM, Xing YM and Guo SX 2015. Habitat suitability assessment of medicinal *Polyporus umbellatusin* China based on Maxent modelling. *Zhongguo Zhong Yao Za Zhi* **40**(14): 2792-2795.

Magday J, Bungihan M and Dulay R 2017. Optimization of mycelial growth and cultivation of fruiting body of Philippine wild strain of *Ganoderma lucidum*. *Current Research in Environment and Applied Mycolcology* **4**(2): 162-172.

Mathur M 2014. Spatio-temporal variability's in distribution patterns of *Tribulus terrestris*: Linking patterns and processes. *Journal of Agricultural Science and Technology* **16:** 1187-1201.

Mathur M and Sundaramoorthy S 2019. Woody perennial diversity at various land forms of the five agro-climatic zones of Rajasthan, India. In: *Biodiversity and Chemotaxonomy. Sustainable Development and Biodiversity,* Ramawat K. (eds) vol 24. Springer, Cham. https://doi.org/10.1007/978-3-030-30746-2_5. Print ISBN 978-3-030-30745-5. Online ISBN 978-3-030-30746-2.

Mathur M and Sundarmoorthy S 2013. Inter-specific association of herbaceous vegetation in semi-arid thar desert, India. *Range Management and Agroforestry* **34**(1): 26-32.

Mawar R, Ram L, Deepesh and Mathur T 2020. *Gandoderma*. In: *Beneficial Microbes in Agro-Ecology* Amaresan N., Kumar M. S., Annapurna K., Kumar, K. and Sankaranarayanan, A. Academic Press, Elsevier, United Kingdom. ISBN: 978-0-12-823414-3 https://doi.org/10.1016/B978-0-12-823414-3.00031-9

Meehan K 2015. *Composition to Promote Hair Growth in Humans*. U.S. Patent US9144542.

Miyamoto Y, Sakai A, Hattori M and Nara K 2015. Strong effect of climate on ectomycorrhizal fungal composition: Evidence from range overlap between two mountains. *Internal Society for Microbial Ecology* **9**: 1870-1879.

Naher L, Yusuf UK, Ismail A, Tan S and Mondal MMA 2013. Ecological status of *Ganoderma* and basal stem rot disease of oil palms (*Elaeis guineensis* Jacq.). *Australasian Journal of Crop Science* **7**(11): 1723-1727.

Obiakara MC and Fourcade Y 2018. Climatic niche and potential distribution of *Tithonia diversifolia* (Hemsl.) A. Gray in Africa. *PLoS ONE* **13**(9): e0202421.

Oei P 2003. *Mushroom Cultivation: Appropriate Technology for Mushroom Growers*. Backhuys Publishers

Oke Olaya G and Abawi GS 1996. Effect of water potential on mycelial growth and on production and germination of sclerotia of *Macrophomina phaseolina*. *Plant Disease* **80:** 1347-1350.

Osorio-Olivera L, Lira-Noriega A, Soberon J, Townsend PA, Facon M, Contreas Diaz RG, Martinez-Meyer E, Barve V and Barve N 2020. Ntbox: An R package with graphical user interface for modelling and evaluating multidimensional ecological niches. *Methods in Ecology and Evolution* **11**: 1199-1206.

Padalia H, Srivastava V and Kushwaha SPS 2014. Modelling potential invasion range of alien invasion species, *Hyptis suaveolens* (L) in India: Comparison of MaxEnt and GARP. *Ecological Informatics* **22**: 36-43.

Pathak PS 1986. Mortality in leucaena due to *Ganoderma lucidum*. *Leucaena Research Report* 7: 65

Phillips SJ and Dudik M 2008. Modelling of species distributions with Maxent: New extensions and a comprehensive evaluation. *Ecography* **31**: 161-175.

Phillips SJ, Anderson RP and Schapire RE 2006. Maximum entropy modelling of species geographic distributions. *Ecological Modelling* **190**: 231-259.

Pietras M, Litkowiec M and Golebiewska J 2018. Current and potential distribution of the ectomycorrhizal fungus *Suillus lakei* ((Murrill) A.H. Sm. & Thiers) in the invasion range. *Mycorrhiza* **28**: 467-475.

Pilotti CA 2005. Stem rots of oil palm caused by Ganoderma boninense: Pathogen biology and epidemiology. *Mycopathologia* **159** (1): 129-137.

Raina AK 1983. Performance of leucaena in the Indian arid zones. 3. *Fusarium* gummosis and *Ganoderma* root rot. *Leucaena Research Report* **4**: 35-36.

Ramankutty N, Evan AT, Monfreda C and Foley JA 2010a. *Global Agricultural Lands: Croplands, 2000*. Data distributed by the Socioeconomic Data and Applications Centre (SEDAC): http://sedac.ciesin.columbia.edu/es/aglands.html.

Ramankutty N, Evan AT, Monfreda C and Foley JA 2010b). *Global Agricultural Lands: Pastures, 2000*. Data distributed by the Socioeconomic Data and Applications Center (SEDAC): http://sedac.ciesin.columbia.edu/es/aglands.html

Sankaran KV, Bridg, PD and Gokulapalan C 2005. *Ganoderma*

diseases of perennial crops in India: An overview. *Mycopathologia* **159**: 143-152.

Schenk HJ and Jackson RB 2009. ISLSCP II Ecosystem Rooting Depths. In *Hall, Forrest* G., G. Collatz, B. Meeson, S. Los, E. Brown de Colstoun, and D. Landis (eds.). ISLSCP Initiative II Collection. Data set. Available on-line [http://daac.ornl.gov/] from Oak Ridge National Laboratory Distributed Active Archive Center, Oak Ridge, Tennessee, U.S.A. doi:10.3334/ORNLDAAC/929

Schuch UK and Kelly JJ 2007. Mesquite trees for the urban landscape, Bulletin of the Desert. Legume Program of the Boyce Thompson Southwestern Arboretum **19**(2): The University of Arizona, Tucson

Shah KK, Tiwari I, Modi B, Pandey HP, Subedi S and Shrestha J 2021. Shisham (*Dalbergia sisso*) decline by dieback disease, root pathogens and their management: S review. *Journal of Agriculture and Natural Resources* **4**(2): 255-272.

Singh SK, Doshi A and Pancholy A 2013. Biodiversity in wood–decay macro–fungi associated with declining arid zone trees of India as revealed by nuclear rDNA analysis. *European Journal of Plant Pathology* **136**: 373-382.

Stojek K, Gillerot L and Jaroszewicz B 2022. Predictors of mushroom production in the European temperate mixed deciduous forest. *Forest Ecology and Management* **522:** 120451.

Subedi K, Basnet BB, Pandey R, Neupane M and Tripathi GR 2021. Optimizatin of growth condition and biological activities of Nepalese *Ganoderma lucidum* strain Philippine. *Advances in Pharmacological and Pharmaceutical Sciences* https://doi.org/10.1155/2021/4888979

Sudheer SI, Alzorqi S, Manickam and Al A 2019. Bioactive compounds of the wonder medicinal mushroom Ganoderma lucidum in *Bioactive Molecules in Food*, J.-M. M´erillon and K. G. Ramawat, Eds., Springer International Publishing, Cham, Switzerland, pp. 1863-1893.

Taofiq O, González-Paramás AM, Martins A, Barreiro MF and Ferreira ICFR 2016. Mushrooms extracts and compounds in cosmetics, cosmeceuticals and nutricosmetics:A review. *Industrial Crops Production* **90**: 38-48.

Tattar TA 1989. *Diseases of Shade Trees.* Academic Press. Sand Diego, California. P. 391.

Tesfaw A, Tadesse A and Kiros G 2015. Optimization of oyster (*Pleurotus ostreatus*) mushroom cultivation using locally available substrates and materials in Debre Berhan, Ethiopia. *Journal of Applied Biology and Biotechnology***3** (1): 15-20.

Van Geel, M, Jacquemyn H, Plue J, Saar L, Kasari L, Peeters G, van Acker K, Honnay O and Ceulemans T 2018. Abiotic rather than biotic filtering shapes the arbuscular mycorrhizal fungal communities of European seminatural grasslands. *New Phytol* **220**: 1262–1272.

Vetrovsky T, Kohout P, Kopecky M, Machac A, Man M, Bahnmann B.D. Brabcova V, Choi, J, Meszarosova L, Human ZR, Lepinay C, Llado S, Lopez-Mondejar R, Martinovic T, Masinova T, Morais D, Navratilova D, Odriozola I, Stursova M, Svec K, Tlaskal V, Urbanova M, Wan J, Zifcakova L, Howe A, Ladau J, Peay KG, Storch D, Wild J and Baldria P 2019. A meta-analysis of global fungal distribution reveals climate-driven pattern. *Nature Communications* **10**: 5142 | https://doi.org/10.1038/s41467-019-13164-8

Wang R, Li Q, He S, Liu Y, Wang M and Jiang G 2018. Modelling and mapping the current and future distribution of *Pseudomonas syringae pv*. *actinidiae* under climate change in China. *PLoS ONE* **13**(2): e0192153.

Wang XC, Xi RJ, Li Y, Wang DM and Yao YJ 2012. The Species Identity of the Widely Cultivated Ganoderma, 'G. lucidum' (Lingzhi), in China. *PLoS ONE* **7**(7): e40857.

Wang Y, Xie B, Wa F, Xiao Q and Dai L 2007. Application of ROC curve analysis in evaluating the performance of alien species' potential distribution models. *Biodiversity Science* **15:** 365-372.

Watt MS, Ganley RJ, Kriticos DJ and Manning LK 2011. Dothistroma needle blight and pitch canker: The current and future potential distribution of two devastating diseases of Pinus species. *Canadian Journal of Forestry Research* **41**(2): 412-424.

Watt MS, Kriticos DJ, Alcaraz S, Brown AV and Leriche A 2009. The hosts and potential geographic range of Dothistroma needle blight. *Forest Ecology and Management* **257**(6): 1505-1519.

Wright AN, Schwartz MW, Hijmans RJ and Shaffer HB 2016. Advances in climate models from CMIP3 to CMIP5 do not change predictions of future habitat suitability for California reptiles and amphibians. *Climate Change* **134**: 579-591.

Wu Y, Choi MH, Li J, Yang H and Shin HJ 2018. Mushroom cosmetics: The present and future. *Cosmetics* **3:** 22.

Yang Y, Zhang H, Gong X, Yi F, Zhu W and Li L 2019. Advance in research on the active constituents and physiological effects of *Ganoderma lucidum. Biomedical Dermatology* **3**: 6.

Yonow T, Hattingh V and de Villiers M 2013. CLIMEX modelling of the potential global distribution of the citrus black spot disease caused by *Guignardia citricarpa* and the risk posed to European. *Journal of Crop Protection* https://doi.org/10.1016/j.cropro.2012.10.006

Yuan HS, Wei Y, Zhou L, Qin W, Cui B and He S 2019. Potential distribution and ecological niches of four butt-rot pathogenic fungi in Northeast China. *Biodiversity Science* **27**(8): 873-879.

Zhao Y, Zhao M, Zhang L, Wang C and Xu Y 2021. Predicting possible distribution of tea (*Camellia sinensis* L.) under climate change scenarios using MaxEnt Model in China. *Agriculture* **11:** 1122.

Zhou LW, Cao Y, Wu SH, Vlasak J, Li DW, Li MJ and Dai YC 2015. Global diversity of the *Ganoderma lucidum* complex (Ganodermataceae, Polyporales) inferred from morphology and multilocus phylogeny. *Phytochemistry* **114**: 7-15.

Received 22 August, 2022; Accepted 26 February, 2023